*Advanced Materials Research Vol. 770 (2013) pp 331-334*
*© (2013) Trans Tech Publications, Switzerland*
*doi:10.4028/www.scientific.net/AMR.770.331*

# Effects of Thermal and Cross-Track Variations for Longitudinal Heat-Assisted Magnetic Recording Systems

Piya Kovintavewat, Adisorn Kaewpukdee, and Nitthita Chirdchoo

Data Storage Technology Research Center, Nakhon Pathom Rajabhat University
Nakhon Pathom, 73000, Thailand

piya@npru.ac.th, adisorn@npru.ac.th, nitthita@npru.ac.th

**Keywords:** Longitudinal HAMR system, Thermal and cross-track variation, Transition characteristics

**Abstract.** The current data recording technology is approaching its capacity limit approximately 1 Tbit/in$^2$ (terabits per square inch) known as superparamagnetic limit. Heat-assisted magnetic recording (HAMR) is one of the promising technologies that is being planned to be used as a new data recording technology to achieve the storage capacity beyond 1 Tbit/in$^2$. In HAMR, the laser is applied to heat a magnetic medium during the writing process, which results in the unique transition characteristics if compared to a conventional system. This paper investigates the effects of thermal and cross-track variations to the transition characteristics (both transition center and transition parameter) of longitudinal HAMR systems. Experimental results indicate that the longitudinal HAMR system can withstand some amount of thermal and cross-track variations and still provides satisfactory system performance.

## Introduction

Current hard disk drives (HDDs) are based on a perpendicular recording technology, whose storage capacity is reaching the superparamagnetic limit of 1 Tbit/in$^2$ [1]. HAMR is one of the promising technologies that can achieve the storage capacity beyond 1 Tbit/in$^2$, and is expected to be employed as the next recording technology because of its feasibility to cooperate with the current HDDs. A simple way to increase the storage capacity is to reduce a volume of a grain size ($V$) required for storing a single bit in magnetic medium. Practically, a magnetic grain is characterized by its uniaxial anisotropy coefficient ($K_u$), where the higher the $K_u$, the harder the change of medium magnetization. In general, the magnetic grain is *stable* when the magnetic energy ($K_uV$) is much greater than (e.g., ≥ 60) the thermal energy ($k_BT$) [2], where $k_B = 1.38\times10^{-23}$ is a Boltzmann's constant and $T$ is a temperature in Kelvin. Thus, reducing $V$ means $K_u$ must be increased so as to keep $K_uV$ constant. Unfortunately, increasing $K_u$ results in the higher magnetic field needed to change the direction of medium magnetization. However, in HAMR, the medium is heated so that a lower magnetic field can be used to write a data bit into a medium. After the data bit has been written, the medium is rapidly cooled down until it reached the ambient temperature. This guarantees the thermal stability of the data bit stored in the medium.

Many papers have investigated the behavior of HAMR systems [2-6]. Rausch *et al.* [2] proposed a thermal Williams-Comstock model (TWCM) to study the transition characteristics of longitudinal HAMR systems, which concluded that many parameters (e.g., alignment, write current, and laser power) are needed to be optimized to achieve high performance in HAMR implementation. The effects of cross-track transition location and transition parameter in longitudinal HAMR systems were investigated in [3]. The variation of transition responses of HAMR systems as a function of laser spot positions was studied in [4]. Furthermore, the effects of several crucial parameters (e.g., peak temperature, medium coercivity ($H_c$), write head gap, deep gap field, and fly height) were investigated in longitudinal HAMR systems [5, 6].

This paper uses the TWCM and a microtrack model to study how the thermal (peak temperature) and cross-track variations affect the behavior of transition characteristics (i.e., a transition center and a transition length) in longitudinal HAMR systems [2, 6]. This study will serve as a guideline for a system designer to carefully design the HAMR system to avoid these variations so as to obtain the best system performance.

**A Williams-Comstock Thermal Model and a Microtrack Model**

An analytical expression known as a Williams-Comstock model [3] can be utilized to study the transition characteristics of longitudinal magnetic recording systems. Then, Rausch *et al.* [2] include the thermal gradient into this model to capture the effect of temperature variations on $H_c$ and the remanent magnetization ($M_r$) of the medium, resulting in the TWCM given by

$$\left.\frac{dM(x)}{dx}\right|_{x_0} = \left.\frac{dM(H_{tot})}{dH_{tot}}\right|_{H_c(T_0)} \left[ \left.\frac{dH_h(x)}{dx}\right|_{x_0} + \left.\frac{dH_d(x)}{dx}\right|_{x_0} - \left.\frac{dH_c(T_0)}{dT}\right|_{T_0} \left.\frac{dT}{dx}\right|_{x_0} \right], \tag{1}$$

where $H_{tot}$ is total applied field, $H_h$ is head field, $H_d$ is demagnetization field, $M$ is medium magnetization, and $T(x)$ is the temperature profile in a medium. Here, we consider the large spot thermal recording where the thermal gradient and the effect of the demagnetization field are small. Therefore, a transition from $-M_r$ to $+M_r$ is assumed to occur when the total applied field $H_{tot} = H_h$ is equal to coercivity $H_c$, i.e.,

$$H_c\left(T\left(x_0\right)\right) \approx H_h\left(x_0\right). \tag{2}$$

Generally, Eq. 2 can be solved numerically for the transition center ($x_0$), while Eq. 1 is used to solve for the transition parameter ($a$), where the transition length is defined as $\pi a$ [2]. Hence, both the $x_0$ and $a$ can completely characterize the HAMR system. To solve Eq. 2, each term in Eq. 2 is needed to be evaluated, which can be found analytically in [2, 6].

In practice, TWCM is insufficient for describing the HAMR process because it ignores cross-track variations in the transition. Since the thermal profile is assumed to be Gaussian, there is not only an along-track variation in $H_c$, but also a cross-track variation. To account for these variations, a micro-track model must be used to approximate the transition curvature [2]. Specifically, a magnetic track is divided into $N$ subtracks with equal width. Accordingly, the TWCM is applied for each subtrack to determine $x_0$ and $a$. The transition responses of each subtrack are adequate to determine the characteristics of HAMR system. If the system response of an individual microtrack is $h(a, t)$, the total response for the whole track will be expressed as [2]

$$p(t) = \frac{1}{N}\sum_{i=1}^{N} h\left(a_i, t-\tau_i\right) \tag{3}$$

where $h(t)$ is the microtrack response, $a_i$ is the transition parameter, and $t-\tau_i$ is a relative location of the transition center for the $i$-th subtrack.

**Experimental Results**

Table 1 illustrates the parameter settings used to investigate the transition characteristics of the longitudinal HAMR system. To study the effect of thermal (peak temperature) variation, we assume that the peak temperature $T_{\text{peak}}$ used to heat the medium is a Gaussian random process with mean $T_p$ = 400 °C and a standard deviation of $\sigma$. In this study, we set $\sigma = 2(1 \pm x/100)$ to capture the peak temperature variation of $x$%, and truncate the resulting peak temperature to $T_{\text{peak}} \pm 20$ °C.

Table 1. Parameter settings

| Parameter | Value |
|---|---|
| Coercivity ($H_c$) | -2000 $T(x)$ + 16×10⁵ [A/m] |
| Remanant magnetization ($M_r$) | -1200 $T(x)$ + 12×10⁵ [A/m] |
| Coercive squareness | 0.7 |
| Medium thickness | 20 [nm] |
| Write head gap ($g$) | 100 [nm] |
| Deep gap field | 19×10⁵ [A/m] |
| Read head gap | 5 [nm] |
| Fly height ($d$) | 0 [nm] |
| Width of the track | 120 [nm] |
| Number of subtracks ($N$) | 17 |

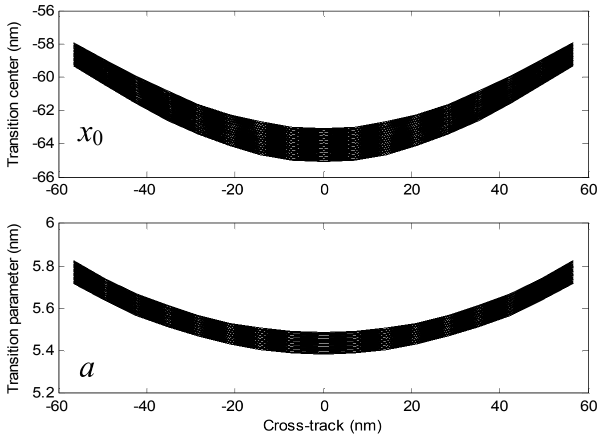


Fig. 1. The transition center and the transition parameter with 10% peak temperature variation.

Table 2. The averaged $x_0$ and $a$ (in nm) for different thermal (peak temperature) variations

| | | Percentage of variation | | | |
|---|---|---|---|---|---|
| **1-st subtrack** | | **0%** | **3%** | **5%** | **10%** |
| mean | $x_0$ | -58.643 | -58.642 | -58.643 | -58.642 |
| | $a$ | 5.768 | 5.768 | 5.768 | 5.769 |
| std. | $x_0$ | 0.000 | 0.110 | 0.137 | 0.154 |
| | $a$ | 0.000 | 0.00069 | 0.00086 | 0.00096 |
| **3-rd subtrack** | | **0%** | **3%** | **5%** | **10%** |
| mean | $x_0$ | -60.779 | -60.779 | -60.780 | -60.779 |
| | $a$ | 5.618 | 5.618 | 5.618 | 5.618 |
| std. | $x_0$ | 0.000 | 0.152 | 0.188 | 0.211 |
| | $a$ | 0.000 | 0.00059 | 0.00074 | 0.00083 |
| **9-th subtrack** | | **0%** | **3%** | **5%** | **10%** |
| mean | $x_0$ | -64.088 | -64.089 | -64.090 | -64.089 |
| | $a$ | 5.436 | 5.436 | 5.436 | 5.436 |
| std. | $x_0$ | 0.000 | 0.233 | 0.288 | 0.323 |
| | $a$ | 0.000 | 0.00057 | 0.00071 | 0.00080 |
| **$PW_{50}$** | | **0%** | **3%** | **5%** | **10%** |
| max. [nm] | | 49.774 | 49.833 | 49.833 | 49.833 |
| min. [nm] | | 49.774 | 49.728 | 49.728 | 49.728 |

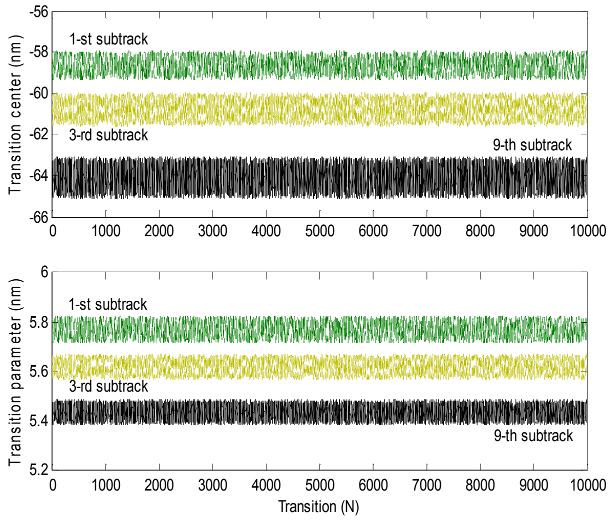


Fig. 2. The transition center and the transition parameter with 10% peak temperature variation at the 1-st, 3-rd, and 9-th subtracks.

Fig. 1 shows the $x_0$ and $a$ for all subtracks when the peak temperature variation is 10%. Clearly, $x_0$ varies within several nanometers, and $a$ also changes only few nanometers. It seems that a small variation is found at the track edge, but a large variation is occurred at the track center. This might be because the laser position is pointed at the track center. To confirm this result, we plot the values of $x_0$ and $a$ at the 1-st, 3-rd and 9-th subtracks for 10000 magnetic transitions in Fig. 2. Again, same result is obtained.

Furthermore, we compute the averaged transition center $x_0$ and the averaged transition parameter $a$ in Table 2 for different peak temperature variations (average based on 17 subtracks) to understand the behavior of $x_0$ and $a$, where $PW_{50}$ is the width of the pulse $p(t)$ in Eq. 3 at half its maximum. It is apparent that the mean of $x_0$ and $a$ is almost constant, but the standard deviation (std.) of $x_0$ and $a$ is increased when variation is large. In addition, the std. of $x_0$ and $a$ is getting large when the subtrack is close to the track center (i.e., the 9-th subtrack). We also display the $PW_{50}$ of the total response $p(t)$ in Table 2. It is clear that $PW_{50}$ is not primarily affected by peak temperature variation. Note that the smaller the $PW_{50}$, the higher the achievable storage capacity [2].

Similarly, to study the effect of cross-track variation (i.e., when the write head is moved away from the track center), we plot the values of $x_0$ and $a$ at the 1-st, 3-rd and 9-th subtracks for 10000 magnetic transitions with 10% cross-track variation in Fig. 3. Clearly, the 1-st subtrack experiences the largest variation in $x_0$ and $a$ if compared to the 3-rd and 9-th subtracks because this subtrack is farthest from the track center where the laser is pointed to. Additionally, Table 3 also shows the averaged transition

Table 3. The averaged $x_0$ and $a$ (in nm) for different cross-track variations

| | | Percentage of variation | | | |
|---|---|---|---|---|---|
| **1-st subtrack** | | **0%** | **3%** | **5%** | **10%** |
| mean | $x_0$ | -58.643 | -58.913 | -59.069 | -59.418 |
| | $a$ | 5.768 | 5.747 | 5.735 | 5.710 |
| std. | $x_0$ | 0.000 | 0.026 | 0.072 | 0.265 |
| | $a$ | 0.000 | 0.0001 | 0.0004 | 0.0013 |
| **3-rd subtrack** | | **0%** | **3%** | **5%** | **10%** |
| mean | $x_0$ | -60.779 | -61.014 | -61.148 | -61.438 |
| | $a$ | 5.618 | 5.603 | 5.595 | 5.578 |
| std. | $x_0$ | 0.000 | 0.019 | 0.053 | 0.184 |
| | $a$ | 0.000 | 0.0000 | 0.0004 | 0.0006 |
| **9-th subtrack** | | **0%** | **3%** | **5%** | **10%** |
| mean | $x_0$ | -64.088 | -64.080 | -64.067 | -64.015 |
| | $a$ | 5.436 | 5.436 | 5.437 | 5.439 |
| std. | $x_0$ | 0.000 | 0.000 | 0.0004 | 0.0062 |
| | $a$ | 0.000 | 0.0000 | 0.0000 | 0.0000 |
| **$PW_{50}$** | | **0%** | **3%** | **5%** | **10%** |
| max. [nm] | | 49.774 | 49.845 | 49.901 | 50.039 |
| min. [nm] | | 49.774 | 49.723 | 49.698 | 49.658 |

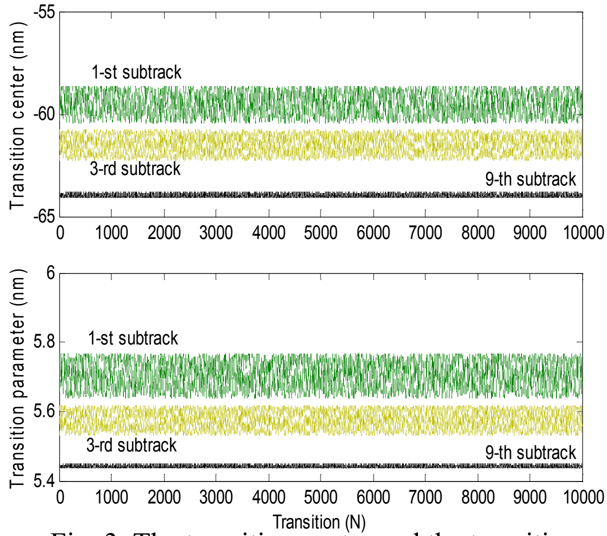


Fig. 3. The transition center and the transition parameter with 10% cross-track variation at the 1-st, 3-rd, and 9-th subtracks.

center $x_0$ and the averaged transition parameter $a$ at different cross-track variations. It is evident that the mean of $x_0$ and $a$ is varied, especially when cross-track variation is large. This can be implied that the cross-track variation has more impact against $x_0$ and $a$ than the peak temperature variation. Moreover, we found that the std. of $x_0$ and $a$ is large when the subtrack is further away from the track center. Again for $PW_{50}$, it seems that $PW_{50}$ is not affected by cross-track variation.

## Summary

This paper investigated the effects of thermal (peak temperature) and cross-track variations on the transition characteristics (i.e., the transition center $x_0$, the transition parameter $a$, and the $PW_{50}$) of the longitudinal HAMR system, based on the TWCM and the microtrack model. Based on our study, it can be concluded that these two variations cause the $x_0$ and $a$ of each subtrack to vary, thus affecting the $PW_{50}$ of the total transition response. In addition, we found that the cross-track variation has more impact against the $x_0$ and $a$ than the peak temperature variation. Consequently, the system designer should carefully design all components to be robust against the thermal and cross-track variations that might occur in the longitudinal HAMR system so as to achieve the best system performance.

## References


[1] Y. Shiroishi, K. Fukuda, I. Tagawa, H. Iwasaki, S. Takenoiri, H. Tanaka, H. Mutoh, N. Yoshikawa, Future options for HDD storage, IEEE Trans. Magn. 45 (2009) 3816-3822.

[2] T. Rausch, J. A. Bain, D. D. Stancil, T. E. Schelesinger, Thermal Williams-Comstock model for predicting transition length in a heat-assisted magnetic recording system, IEEE Trans. Magn. 40 (2004) 137-147.

[3] M. L. Williams, R. L. Comstock, An analytic model of the write process in digital magnetic recording, Proc. 17th Annu. AIP Conf. (1971) 724-738.

[4] M. F. Erden, T. Rausch, W. A. Challener, Cross-track transition location and transition parameter effects in heat-assisted magnetic recording, IEEE Trans. Magn. 41 (2005) 2189-2194.

[5] R. Radhakrishan, M. F. Erden, C. He, B. Vasic, Transition response characteristics of heat-assisted magnetic recording and their performance with MTR codes, IEEE Trans. Magn. 43 (2007) 2298-2300.

[6] A. Kaewpukdee, N. Chirdchoo, P. Kovintavewat, Transition characteristics of longitudinal heat-assisted magnetic recording systems, Procedia Engineering 32 (2012) 315-322.